Journal of Bone Oncology 26 (2021) 100330

Contents lists available at ScienceDirect

Journal of Bone Oncology

journal homepage: www.elsevier.com/locate/jbo

The HMGB1/RAGE axis induces bone pain associated with colonization of 4T1 mouse breast cancer in bone

Tatsuo Okui [a,c], Masahiro Hiasa [b,c], Shoji Ryumon [a], Kisho Ono [a], Yuki Kunisada [a], Soichiro Ibaragi [a], Akira Sasaki [a], G. David Roodman [c,d], Fletcher A. White [e], Toshiyuki Yoneda [c,f,*]

[a] Department of Oral and Maxillofacial Surgery and Biopathology, Okayama University Graduate School of Medicine, Dentistry and Pharmaceutical Science, Okayama, Japan
[b] Department of Biomaterials and Bioengineerings, University of Tokushima Graduate School of Dentistry, Tokushima, Japan
[c] Department of Medicine, Hematology Oncology, Indiana University School of Medicine, Indianapolis, IN, USA
[d] The Rodebusch VA, Indianapolis, IN, USA
[e] Department of Anesthesia, Paul and Carole Stark Neurosciences Research Institute, Indianapolis, IN, USA
[f] Department of Cellular and Molecular Biochemistry, Osaka University Graduate School of Dentistry, Osaka, Japan

ARTICLE INFO

Article history:
Received 26 July 2020
Revised 6 October 2020
Accepted 6 October 2020
Available online 28 October 2020

Keywords:
Breast cancer
Bone pain
Sensory neurons
HMGB1
RAGE

ABSTRACT

Bone pain is a common complication of breast cancer (BC) bone metastasis and is a major cause of increased morbidity and mortality. Although the mechanism of BC-associated bone pain (BCABP) remains poorly understood, involvement of BC products in the pathophysiology of BCABP has been proposed. Aggressive cancers secrete damage-associated molecular patterns (DAMPs) that bind to specific DAMP receptors and modulate cancer microenvironment. A prototypic DAMP, high mobility group box 1 (HMGB1), which acts as a ligand for the receptor for advanced glycation end products (RAGE) and toll-like receptors (TLRs), is increased in its expression in BC patients with poor outcomes. Here we show that 4T1 mouse BC cells colonizing bone up-regulate the expression of molecular pain markers, phosphorylated ERK1/2 (pERK) and pCREB, in the dorsal root ganglia (DRGs) innervating bone and induced BCABP as evaluated by hind-paw mechanical hypersensitivity. Importantly, silencing HMGB1 in 4T1 BC cells by shRNA reduced pERK and pCREB and BCABP with decreased HMGB1 levels in bone. Further, administration of a neutralizing antibody to HMGB1 or an antagonist for RAGE, FPS-ZM1, ameliorated pERK, pCREB and BCABP, while a TLR4 antagonist, TAK242, showed no effects. Consistent with these *in vivo* results, co-cultures of F11 sensory neuron-like cells with 4T1 BC cells in microfluidic culture platforms increased neurite outgrowth of F11 cells, which was blocked by HMGB1 antibody. Our results show that HMGB1 secreted by BC cells induces BCABP via binding to RAGE of sensory neurons and suggest that the HMGB1/RAGE axis may be a potential novel therapeutic target for BCABP.

1. Introduction

Breast cancer (BC) frequently metastasizes to bone, inducing osteolytic metastases accompanied by severe bone pain [1]. BC-associated bone pain (BCABP) is a major cause of increased morbidity and mortality in BC patients [2]. However, currently-available treatments for BCABP are still unsatisfactory and inappropriate [3]. According to the recommendation of the WHO analgesic ladder, opioids are the mainstay of cancer pain management and reasonably control BCABP in BC patients [4]. However, opioid produces troublesome side-effects including cognitive disturbances, sedation, constipation and respiratory depression. Long-term opioid use causes addiction, drug abuse, osteopenia and osteoporosis [5]. Non-steroidal anti-inflammatory drugs are often used for BCABP but their effects are limited due to the short

Abbreviations: ALP, alkaline phosphatase; BC, breast cancer; BCABP, breast cancer-associated bone pain; CGRP, calcitonin gene-related peptide; CM, conditioned medium; CREB, cyclic AMP-responsive element-binding protein; DAMP, damage-associated molecular pattern; DbcAMP, dibutyryl cyclic AMP; DRG, dorsal root ganglion; ERK, extracellular signal-regulated kinase; HMGB1, high mobility group box 1; M-CSF, macrophage colony-stimulating factor; MNOCs, multinucleated osteoclast-like cells; pERK, phosphorylated ERK; pCREB, phosphorylated CREB; RAGE, receptor for advanced glycation end products; RANKL, receptor activator of NF-κB ligand; SN, sensory neuron; TRAP, tartrate-resistant acid phosphatase; TRL, toll-like receptor; 4T1 mice, mice intratibially inoculated with 4T1 BC cells; 4T1/sh control mice, mice intratibially inoculated with 4T1 BC/sh control cells; 4T1/sh HMGB1 mice, mice intratibially inoculated with 4T1 BC/sh HMGB1 cells.

* Corresponding author at: Department of Cellular and Molecular Biochemistry, Osaka University Graduate School of Dentistry, 1-8 Yamadaoka, Suita, Osaka 565-0871, Japan.
E-mail address: tyoneda@dent.osaka-u.ac.jp (T. Yoneda).

https://doi.org/10.1016/j.jbo.2020.100330
2212-1374/

duration of action and lack of long-lasting effects. Further, they have potential adverse effects on renal, gastrointestinal, cardiovascular and hematological systems [3].

Although the mechanism of BCABP remains poorly understood, it has been proposed that the products of the cellular components in the BC microenvironment including metastatic BC cells, stromal cells, immune cells, adipocytes, endothelial cells, and bone cells (osteoclasts, osteoblasts, and osteocytes) induce sensitization and excitation of sensory neurons (SNs) that innervate bone and could contribute to BCABP [6].

Aggressive cancer cells release damage-associated molecular patterns (DAMPs) from the necrotic core in the tumor [7]. Secreted DAMPs then promote the development, progression, and metastasis of cancer by initiating noninfectious inflammatory responses [8]. High mobility group box 1 (HMGB1), which is a highly conserved ubiquitous nuclear non-histone DNA-binding protein and a prototypic member of DAMPs [9], is passively released from dead, dying and injured cells. However, recent reports showed that HMGB1 is also actively secreted from cancer cells in response to various stimuli [10]. Extracellular HMGB1 acts by binding to cell surface receptors such as receptor for advanced glycation end products (RAGE), toll-like receptor 2, 4 and 9 (TLR2, TLR4 and TLR9), syndecan-1, and Mac-1, to propagate inflammatory and pain signals [9,10]. Of note, clinical studies reported that HMGB1 levels are increased in tumor tissue and circulating blood in BC patients with poor outcomes [11]. Recently, HMGB1 was found to mediate inflammatory and immune reactions in nervous systems [12] and implicated in neuropathic and chronic pain [13], leading us to the hypothesis that HMGB1 plays a role in BCABP. To test this hypothesis, we established an animal model of BCABP in which 4T1 mouse BC cells were injected into the bone marrow cavity of tibiae (hereafter these mice are designated as 4T1 mice). BCABP was evaluated by hind-paw mechanical hypersensitivity, a widely-used behavior assay for bone pain in rodents [14] and the expression of phosphorylated extracellular-regulated kinase 1/2 (ERK1/2) and cyclic AMP-responsive element-binding protein (CREB), two molecular markers of pain [15]. Using this model, we found that HMGB1 secreted from BC induced BCABP via activation of RAGE of SNs. We propose that blockade of the HMGB1/RAGE axis may be an effective approach for the treatment of bone pain in patients with advanced BC.

2. Methods

All animal studies were approved by the Institutional Animal Care and Use Committee at Indiana University School of Medicine (Protocol #: 10553) and conducted according to the ARRIVE guidelines.

2.1. Reagents

Anti-RAGE antibody (anti-mouse, monoclonal #sc-80652) was purchased from SantaCruz Biotechnology, (Dallas, TX) anti-TLR4 (anti-mouse, monoclonal #ab22048 anti-HMGB1 antibody (anti-rabbit, monoclonal, ab79823), anti-CGRP antibody (anti-goat, polyclonal, #ab36001) and anti-peripherin antibody (anti-rabbit, #ab4666) were purchased from Abcam (Cambridge, MA). Anti-HMGB1 neutralizing antibody (Chicken IgY, # 326052233) and control antibody (Chicken IgY #326058471) were purchased from Shino test corporation (Tokyo, Japan). Anti-phospho-p44/42 MAPK antibody (anti-rabbit, monoclonal, #4370), anti-p44/42 MAPK antibody (anti-rabbit, monoclonal, #4695), anti-phospho CREB (anti-rabbit, monoclonal, #9198), horseradish peroxidase (HRP)-conjugated IgG antibody (anti-rabbit, monoclonal, #7074), HRP-conjugated IgG antibody (anti-mouse, monoclonal, #7076), anti-mouse IgG (H + L), F(ab′)2 Fragment (Alexa Fluor® 647 Conjugate) #4410, and anti-rabbit IgG (H + L), F(ab')2 Fragment (Alexa Fluor® 488 Conjugate) #4412 were purchased from Cell Signaling Technology (Danvers, MA).

2.2. BC cells

Mouse 4T1 BC cells were obtained from the Human Science Resources Bank (Osaka, Japan) and cultured in DMEM (Thermo Fisher Scientific, Waltham, MA) supplemented with 10% heat-inactivated FBS and 1% penicillin–streptomycin in an atmosphere of 5% CO_2 at 37 °C. Human BC cell lines MDA-MB-231 and MCF-7 were obtained from the American Type Culture Collection (ATCC; Manassas, VA, USA). Cells were analyzed and authenticated by targeted genomic and RNA sequencing.

2.3. SN cells of dorsal root ganglion (DRG)

Primary rat SN cells of DRGs were purchased from Lonza (R-DRG-505, Alpharetta, GA) and cultured in primary neuron growth medium (Lonza, CC-4461) with 2% FBS, L-glutamine, gentamycin sulfate-amphotericin (GA-1000, Lonza, CC-4083) and neural survival factor-1 (NSF-1, Lonza, CC-4323) as per the supplier's guidelines. The rat DRG/mouse neuroblastoma hybrid cell line F11 [16], and immortalized rat DRG neuronal cells 50B11 [17], a generous gift from Dr. Hoke (Department of Neurology, School of Medicine, Johns Hopkins University, Baltimore, MD), were cultured in neurobasal medium (Gibco) supplemented with 10% FBS, 1× B27 supplement (Gibco), 0.2% glucose and 0.5 mM glutamine (neuron growth medium).

2.4. Cell proliferation

Cells were plated in six-well plates at 1×10^5 cells per well. The cell number was counted after 72 h of culture with a TC20 automated cell counter (Bio-Rad, Hercules, CA).

2.5. Neurite outgrowth of SN cells

The F11 or 50B11 SN cells were plated in 48-well plates (1.0×10^4/well) in the neuron growth medium for 24 h and subsequently cultured in the absence or presence of the conditioned medium (CM, 20% v/v) harvested from 4T1 BC cell cultures with or without HMGB1 neutralizing antibody or control IgY antibody for 5 days. Plates were then stained with calcein-acetoxymethyl (AM) (1 μM) for 10 min and the length of all outgrowing fluorescent neurites and the number of fluorescent SN cells in plates were determined using Neuron J software under a fluorescent microscope (Olympus IX71, Tokyo, Japan) as previously described [18]. Neurite outgrowth of SN cells was calculated as length of all outgrowing neurites/number of total SN cells and is shown as μm/SN cell in figures.

2.6. Co-culture of SNs and BC cells in microfluidic culture platform

Induction of neurite outgrowth from F11 SN cells over distances in response to extracellular factors released from 4T1 BC cells was evaluated in microfluidic culture platforms as described [19]. Suspensions of F11 SN cells (10^5 cells/10 μl) was plated into the left channels of the microfluidic culture platform (AXIS™, Millipore, Billerica, MA), and the right channels were filled with neuron growth medium. After 12 h of culture, the medium was removed and 4T1 BC cells (10^6 cells/ml) were plated into the right channels and the microfluidic culture platforms were cultured for an additional 48 h. Non-adhered cells and debris were then washed out with PBS, and the channels labeled with calcein AM. The number of F11 SN cells that exhibited neurite outgrowth longer than 50 μm

toward 4T1 BC cells were scored with a fluorescent microscope using Neuron J software.

2.7. Silencing HMGB1 expression in BC cells

The 4T1 BC cells were infected with 1 μg control short hairpin shRNA or HMGB1 shRNA using a Lenti virus particle transduction system (sc-37983-V, SantaCruz Biotechnology, Dallas, TX). After infection, the cells were cultured in DMEM plus 10% FBS for 5 days in the presence of 2 μg/ml puromycin dihydrochloride for selection of cells that stably expressed the shRNAs.

2.8. Osteoclastogenesis in mouse bone marrow cultures

Osteoclastogenesis in bone marrow macrophage cultures was determined as we described [20]. In brief, four-week-old male C57BL/6 mice were sacrificed by cervical dislocation and bone marrow cells in the femurs and tibiae were harvested by flushing out with phosphate-buffered saline using a 27 gauge needle. The cells were then incubated in α-MEM with 30 ng/ml macrophage-colony-stimulating factor (M-CSF) (R&D System, Minneapolis, MN) for 24 h. Non-adherent cells were transferred to 48-well plates (1×10^5 cells/well) and treated with suboptimal dose of 30 ng/ml M-CSF and 10 ng/ml receptor activator of NF-κB ligand (RANKL) (PEPROTECH, Rocky Hill, NJ) in the absence or presence of 4T1 CM (20%, v/v) and with or without the TLR4 antagonist TAK-242 or RAGE antagonist FPS-ZM1. Following five days of culture, the cells were fixed and stained for tartrate-resistant acid phosphatase (TRAP) using a TRAP/alkaline phosphatase (ALP) Stain Kit (FUJIFILM Wako Pure Chemical Corporation, Osaka, Japan). The number of TRAP-positive multinucleated osteoclast-like cells ($TRAP^+$ MNOCs) (nuclear number > 3) in each well were counted under a microscope.

2.9. Intratibial injection of BC cells in mice

The 4T1 BC cells (1×10^5 cells/10 μl) were inoculated in the bone marrow cavity of right tibiae of 4 to 6-week-old female BALB/c mice (4T1 mice) (Harlan Laboratories, Indianapolis, IN), under general anesthesia with ketamine (Ketaset; 90–150 mg/kg, ip) and xylazine (AnaSed; 5–10 mg/kg, ip) as we described [21]. Sham surgery control mice were injected intratibially with PBS.

2.10. Radiological analysis of osteolytic lesions

Bone destruction in tibiae associated with 4T1 BC colonization was assessed by radiographs. Bones were placed against films (22 × 27 cm; Fuji Industrial Film FR: Fuji Photo Film Co., Tokyo) and exposed to soft X-rays at 35 kV for 15 s with a Sofron apparatus (Sofron, Tokyo, Japan). The area of the radiolucent osteolytic lesions was quantified using Lumina Vision/OL (Mitani, Tokyo, Japan) with a microscope (IX81, Olympus, Tokyo, Japan) as we described [22].

2.11. Evaluation of BCABP by hind-paw mechanical hypersensitivity by von Frey test

Nociceptive behavior of 4T1 mice was evaluated by hind-paw mechanical hypersensitivity by the von Frey test using the Dynamic Plantar Aesthesiometer (Ugo Basile, Gemonio, VA, Italy) (Fig. 1A, left) as we described [23]. The von Frey test has been widely used for pain assessment in rodents [14]. This test determines a rodent sensitivity to mechanical stimuli using von Frey filament. Prior to undergoing a pain behavioral test, mice were acclimatized to the environment and facilities for 5–7 days. The hind-paws of animals standing on an elevated mesh platform (Fig. 1A left) are poked by a single von Frey filament with automated increasing force (Fig. 1A, right), so that the force by which animals are induced to show hind-paw withdrawal can be quantitatively estimated. The force is shown as paw withdrawal threshold (g) in figures. Rodents with pain exhibit paw withdrawal with lighter force than those without pain. The test was performed prior to 4T1 BC cell injection to determine the baseline pain behaviors of mice, and every 3–4 days following intratibial injection of 4T1 BC cells until the end of the experiment. Intratibial injection of 4T1 BC cells and von Frey test were performed by researchers who were blinded to the experiments.

2.12. Harvest of DRGs, tibiae, sera and bone marrow fluids

Whole blood was collected by cardiac puncture under general anesthesia. Mice were then sacrificed by cervical dislocation and lumbar DRGs (L3–L5) and tibiae were harvested. The lumbar DRGs were immediately homogenized in RIPA lysis buffer with 1 mM phenylmethylsulfonyl fluoride (PMSF) and phosphatase inhibitors (Na_3VO_4 and NaF). The lysates were centrifuged at 15,000*g* for 5 min at 4 °C, and the supernatants collected. Some DRGs were fixed in 10% neutral-buffered formalin and embedded in paraffin for subsequent histological analyses.

For collection of bone marrow fluids from tibiae, muscles and connective tissues were removed, both ends of tibiae were cut, and whole bone marrow was flushed out with 100 μl PBS, the tubes centrifuged, and the supernatants collected.

2.13. Immunoblotting for phosphorylated extracellular signal-regulated kinase (pERK) and cyclic AMP responsive element-binding protein (pCREB)

DRG lysates were mixed with 4× Laemmli sample buffer (Bio-Rad Laboratories, Hercules, CA), heated at 95 °C for 5 min, electrophoresed in 4–12% SDS-PAGE gels. Proteins were transferred onto PVDF membranes (Bio-Rad), incubated with primary and secondary antibodies according to the Trans-Blot turbo transfer system protocol (Bio-Rad) to detect secondary antibody binding. Antibodies against HMGB1 (1:1000), pERK (1:1000), ERK (1:1000), pCREB (1:1000), and CREB (1:1000) were used as primary and HRP-conjugated anti-rabbit antibody (1:2000) and HRP-conjugated anti-mouse antibody (1:2000) as secondary. Immunoblots were analyzed by Image J software.

2.14. Histologic analysis of bone

Tibiae were harvested, fixed in 10% neutral buffered formalin for 48 h, decalcified in 10% EDTA for two weeks, embedded in paraffin, sectioned and stained with hematoxylin and eosin (HE).

2.15. TRAP staining of tibiae of 4T1 mice

Bone sections were stained for TRAP using a TRAP & ALP double-stain Kit (Takara Bio, Mountain View, CA) and analyzed for osteoclastic bone destruction using Magnafire 4.1 software (Optronics, Goshen, IN) under a microscope (IX81, Olympus). $TRAP^+$OCs were counted at tumor-bone interface at endocortical bone using three levels of sections for each sample according to the methods previously reported [24]. Data are expressed as the number of osteoclasts/bone surface (mm) (No. OC/BS/mm).

2.16. Immunofluorescence

Immunofluorescence analysis was used to determine the expressions of peripherin and RAGE and TLR4 in DRGs from each group of mice. The specimens were incubated with 3% bovine

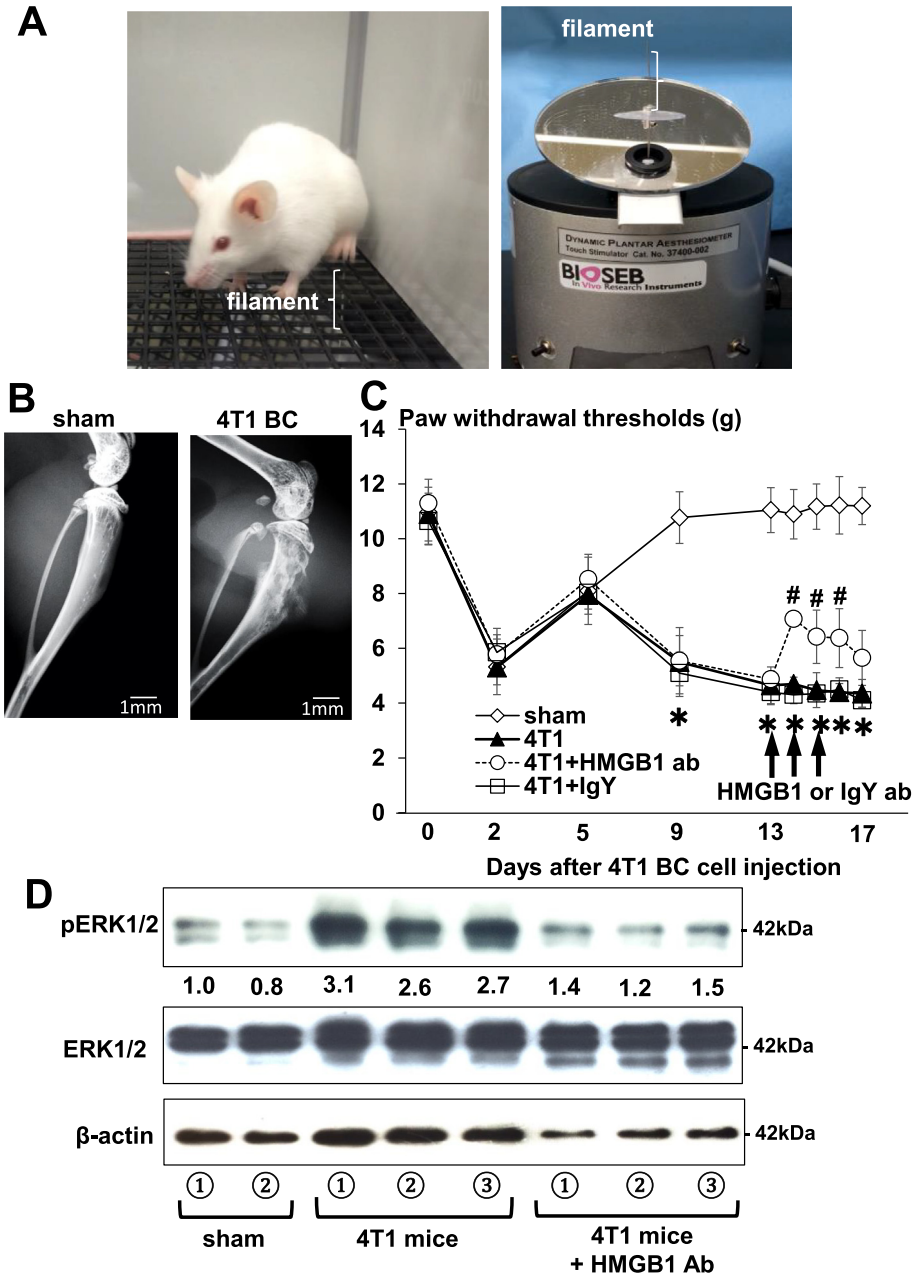

Fig. 1. A mouse model of BCABP. (A) Assessment for hind-paw mechanical hypersensitivity in tibiae of mice by von Frey test. Picture of a mouse withdrawing left hind-leg following poking with von Frey filament (left). The dynamic plantar aesthesiometer with von Frey filament that pokes mouse hind-paw with automated increasing force (right). Mice with pain exhibit hind-paw withdrawal with lighter force than those without pain. (B) Radiograph of osteolytic lesions in tibiae associated with 4T1 BC colonization at day 15 of intratibial cell inoculation (1×10^5 cells/10 μl) in sham (left) and 4T1 mouse (right). Multiple osteolytic lesions are seen in tibiae of 4T1 mouse (right). Scale bar 1 mm. (C) Progression of hind-paw mechanical hypersensitivity in tibiae of 4T1 mice. The force of the filament by which mice withdrew their hind-paw is shown on Y-axis as paw withdrawal thresholds (g) in figure. Mice with BCABP in tibiae show decreased paw withdrawal threshold in parallel with the extent of BCABP. For example, sham mice withdrew their hind-leg by the force of 10.78 ± 1.08 g (Mean ± SD), while 4T1 mice by 5.5 ± 1.45 g (Mean ± SD) at day 9. Decreased paw withdrawal threshold in all group of mice at day 2 is due to surgical trauma. To evaluate therapeutic effects, the neutralizing antibody to HMGB1 (2 mg/kg/mouse, ip, once a day) or control IgY antibody was given at day 13, 14 and 15 (arrows) when 4T1 mice demonstrated considerable hind-paw mechanical hypersensitivity with clearly discernible osteolysis in tibiae associated with 4T1 BC colonization on radiographs. The HMGB1, but not IgY control, antibody significantly reduced hind-paw mechanical hypersensitivity in tibiae of 4T1 mice. Mice withdrew their hind-leg by the force of 4.85 ± 0.22 g (Mean ± SD) before administration of the HMGB1 antibody and by 7.07 ± 0.26 g (Mean ± SD) after administration of the HMGB1 antibody. Data are shown as mean ± SD (n = 8). * Significantly different from sham mice ($p < 0.05$). # Significantly different from 4T1 and 4T1 + IgY mice ($p < 0.05$). (D) Expression of a molecular pain marker pERK in DRGs harvested from sham and 4T1 BC mice treated with or without the HMGB1 antibody. After sacrifice at day 17, DRGs were harvested, immediately lysed and subjected to Western analysis. Expression of pERK was increased in 4T1 mice with BCABP. Administration of the HMGB1 antibody reduced pERK expression in DRGs of 4T1 mice. ERK1/2 expression was not changed.

serum albumin–phosphate buffered saline (BSA–PBS) blocking solution, and then with mouse anti-RAGE (1:100) and mouse anti-TLR4 antibody (1:100) and rabbit anti-peripherin (1:100) antibody overnight at 4 C as primary antibodies, followed by Alexa Fluor 647 anti-mouse IgG (1:1000) and Alexa Fluor 488 anti-rabbit IgG (1:1000) as secondary antibodies.

2.17. Tissue microarrays

HMGB1 expression in human BCs and normal breast tissue was determined using tissue microarrays (#BRM971; US Biomax, Rockville, MD). The antigen was activated by cooking in a citric acid solution. For immunohistochemical analysis, specimens were

incubated with anti-HMGB1 antibody (1:100) (Abcam, Cambridge, MA) overnight at 4 °C, followed by the treatment with streptoavidin-biotin complex (1:100, EnVision System labeled polymer, HRP; Dako, Carpinteria, CA) for 60 min, and visualized with the use of a DAB substrate-chromogen solution (Dako Cytomation Liquid DAB Substrate Chromogen System). Quantification was performed using a BZ-X800 analyzer hybrid cell count system (Keyence, Osaka, Japan), and the relative integrated density was calculated as number of HMGB1-positive BC cells/specimen or/number of total BC cells × 100.

2.18. Determination of HMGB1 levels

HMGB1 levels in the circulating blood and bone marrow fluids of tibiae were determined by ELISA (Shino test, Tokyo) according to the manufacturer's instructions.

2.19. Statistical analysis

Data were analyzed using an unpaired Student's *t*-test for comparisons of two groups and by performing a two-way analysis of variance (ANOVA) and a post hoc Tukey's test for the analysis of multiple group comparisons, using SPSS statistical software, ver. 10. Results are expressed as the mean ± standard deviation (SD). Probability (p) values <0.05 were considered significant.

3. Results

3.1. Mouse model of BCABP

We first characterized 4T1 mice to evaluate if the model is suitable for our study. Mouse 4T1 BC cells injected into the marrow cavity of tibiae showed aggressive growth with extensive osteolytic lesions in 4T1 mice (Fig. 1B, right). The 4T1 mice exhibited time-dependent progressive hind-paw mechanical hypersensitivity (Fig. 1C). [At day 9, sham control and 4T1 mice withdrew their hind-paw by 10.78 ± 1.08 g (Mean ± SD) and 5.5 ± 1.45 g (Mean ± SD) threshold in von Frey test, respectively. These results suggest that 4T1 mice had BCABP. In addition, DRGs harvested from these 4T1 mice showed increased expression of pERK1/2 (Fig. 1D), which is a molecular pain marker [15]. These results indicate that 4T1 mice represent an animal model that allows us to perform quantitative and objective analysis of BCABP.

3.2. Role of HMGB1 in BCABP in 4T1 mice

To determine the role of HMGB1 in BCABP, we next examined the effects of administering a neutralizing antibody to HMGB1 on BCABP in 4T1 mice. Previous studies reported that this neutralizing antibody reduced mortality in mice with pneumococcal meningitis [25] and prevented oxaliplatin-induced peripheral neuropathy in mice [26]. To determine the therapeutic effects, the HMGB1 antibody was administered (2 mg/kg/mouse, ip, once a day) to 4T1 mice at day 13, 14, and 15 when 4T1 mice demonstrated considerable hind-paw mechanical hypersensitivity with clearly discernible osteolysis in tibiae on radiographs. In preliminary experiments, we found that one single injection of the HMGB1 antibody significantly reduced BCABP in 4T1 mice. Therefore, the antibody was scheduled to be administered three consecutive days to ensure the effects on BCABP. Further, since a previous study reported that repeated administrations of the anti-HMGB1 neutralizing antibody for long period of time inhibit osteoclastic bone resorption [27], which substantially contributes to the induction of BCABP [2,28], we attempted to limit the dose of the antibody as small as possible to minimize the effects of the antibody on bone resorption to evaluate the role of HMGB1 per se in BCABP unassociated with bone resorption. We found that the antibody significantly reduced hind-paw mechanical hypersensitivity. Mice withdrew their hind-paw by the force of 4.85 ± 0.22 g (Mean ± SD) before administration of the HMGB1 antibody and by 7.07 ± 0.26 g (Mean ± SD) after administration of the HMGB1 antibody (Fig. 1C), demonstrating that the HMGB1 antibody relieved BCABP in 4T1 mice. The antibody also decreased pERK1/2 expression in DRGs harvested from 4T1 mice (Fig. 1D). Control IgY antibody showed no effects on BCABP (Fig. 1C). These results suggest that HMGB1 plays a critical role in the induction of BCABP and SN activation in 4T1 mice.

We then examined if 4T1 BC express HMGB1 by Western analysis and verified that 4T1 BC, as well as MDA-MB-231 and MCF-7 human BC cells, express HMGB1 (Fig. 2A). Further, ELISA showed that HMGB1 levels in the bone marrow of tibiae injected with 4T1 BC cells were elevated compared to sham surgery mice (Fig. 2B), demonstrating that 4T1 BC cells secrete HMGB1 *in vivo* as well. Of note, serum levels of HMGB1 were not significantly different between sham surgery mice and 4T1 mice (Fig. 2C), suggesting that HMGB1 secretion by 4T1 BC cells in tibiae is not sufficient enough to elevate circulating levels of HMGB1.

To further determine the role of HMGB1 produced by 4T1 BC in the induction of BCABP, 4T1 BC cells in which HMGB1 was silenced by knockdown by sh HMGB1 (4T1/sh HMGB1 cells) were generated and intratibially inoculated in mice (4T1/sh HMGB1 mice). Knockdown of HMGB1 in 4T1/sh HMGB1 cells was validated by western analysis (Fig. 2D). Silencing HMGB1 did not change cell proliferation of 4T1 BC cells in monolayer culture (data not shown). HMGB1 levels in the bone marrow of tibiae, however, were significantly decreased in 4T1/sh HMGB1 mice compared to 4T1 mice and mice intratibially injected with 4T1/sh control cells (4T1/sh control mice) (Fig. 2B), whereas serum HMGB1 levels were not significantly changed in 4T1/sh HMGB1 mice compared to 4T1 and 4T1/sh control mice (Fig. 2C). Importantly, the expression of molecular pain markers, pERK1/2 and pCREB, in DRGs (Fig. 2E) was decreased in 4T1/sh HMGB1 mice compared to 4T1 and 4T1/sh control mice. More importantly, BCABP evaluated by hind-paw mechanical hypersensitivity was significantly reduced in 4T1/sh HMGB1 mice compared to 4T1 and 4T1/sh control mice (Fig. 2F), i.e. 4T1 mice withdrew their hind-leg by the force of 3.84 ± 0.84 g (Mean ± SD), while 4T1/sh HMGB1 mice by 7.26 ± 0.43 g (Mean ± SD) at day 10. Consistent with these results, immunofluorochemical examination showed that axogenesis of peripherin$^+$ SNs was increased in the bone marrow of tibiae of 4T1 and 4T1/sh control mice (Fig. 2G). In contrast, the axogenesis of peripherin$^+$ SNs was decreased in 4T1/sh HMGB1 mice. Quantitative determination revealed that peripherin$^+$ neurons in tibiae of 4T1 and 4T1/sh control mice are 1.506 ± 0.51% (Mean ± SD) and 1.497 ± 0.52% (Mean ± SD), respectively and 0.496 ± 0.34% (Mean ± SD) in 4T1/sh HMGB1 mice, validating the histological results (Fig. 2H). These results suggest that HMGB1 locally secreted by 4T1 BC cells in the bone marrow of tibiae is responsible for increased axogenesis of SNs in tibiae and induction of BCABP in a paracrine manner.

3.3. Role of HMGB1 receptors, receptor activation glycation products (RAGE) and toll-like receptor 4 (TLR4) in BCABP

To further determine the role of HMGB1 in BCABP, we next examined if SNs in bone express two of the major HMGB1 receptors, RAGE and TLR4. HMGB1 is known to act primarily by binding and activating RAGE and TLR4 [9,10]. Immunofluorochemical examination of tibiae showed that RAGE and TLR4 were expressed on peripherin$^+$ SNs innervating bone (Fig. 3A). We then examined the effects of TAK-242, an antagonist for TLR4 [29], and FPS-ZM1,

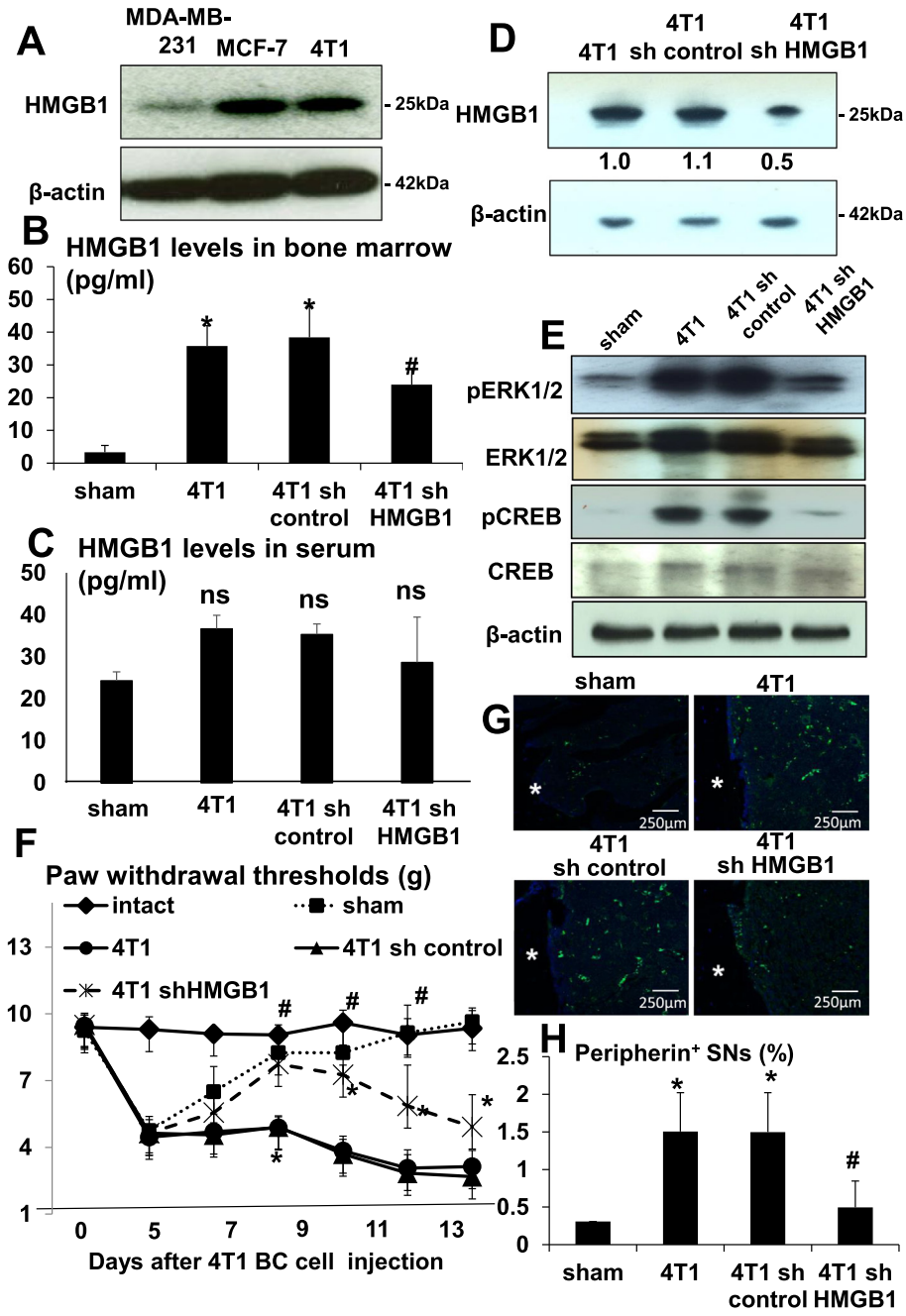

Fig. 2. Role of HMGB1 produced by 4T1 BC in BCABP. (A) Expression of HMGB1 in mouse 4T1 BC and human BC MDA-MB-231 and MCF-7 cells in culture. Whole cell lysates were subjected to Western analysis. HMGB1 levels in the bone marrow of tibiae by ELISA. Bone marrow fluids were collected as described in Methods from sham, 4T1, 4T1/sh control and 4T1/sh HMGB1 mice. (B) HMGB1 levels were increased in the bone marrow of tibiae of 4T1 and 4T1/sh control mice, while significantly decreased in the bone marrow of tibiae of 4T1/sh HMGB1 mice. Data are shown as mean ± SD (n = 8). * Significantly different from sham mice ($p < 0.05$). # Significantly different from 4T1 and 4T1/sh control mice ($p < 0.05$). (C) HMGB1 levels in circulating serum determined by ELISA. Sera were collected as described in Methods from sham, 4T1, 4T1/sh control and 4T1/sh HMGB1 mice. There was no difference in serum levels of HMGB1 among 4T1, 4T1/sh control and 4T1/sh HMGB1 mice. Data are shown as mean ± SD (n = 8). ns: not significantly different from sham. (D) Knockdown of HMGB1 by shRNA in 4T1 BC cells. HMGB1 expression was evaluated by Western analysis in parental 4T1 BC, 4T1/sh control and 4T1/sh HMGB1 cells. HMGB1 expression is successfully reduced in 4T1/sh HMGB1 cells. (E) Expression of molecular pain markers pERK1/2 and pCREB in DRGs of sham, 4T1, 4T1/sh control and 4T1/sh HMGB1 mice. DRGs were harvested after sacrifice at day 15, immediately lysed and subjected to Western analysis. Expression of pERK1/2 and pCREB was increased in DRGs of 4T1 and 4T1/sh control mice compared to sham mice and decreased in DRGs of 4T1/sh HMGB1 mice compared to 4T1 and 4T1/sh control mice. Expression of ERK1/2 and CREB was not changed. (F) Progression of hind-paw mechanical hypersensitivity in tibiae of intact, sham, 4T1, 4T1/sh control and 4T1/sh HMGB1 mice. Sham mice showed hind-paw mechanical hypersensitivity until surgical trauma healed. 4T1 mice withdrew their hind-leg by the force of 3.84 ± 0.84 g (Mean ± SD), while 4T1/sh HMGB1 mice by 7.26 ± 0.43 g (Mean ± SD) at day 10. Data are shown as mean ± SD (n = 8). * Significantly different from intact and sham mice ($p < 0.05$). # Significantly different from 4T1 and 4T1/sh control mice ($p < 0.05$). (G) Axogenesis of peripherin$^+$ SNs in the bone marrow of tibiae by immunofluorescent staining. Tibiae were harvested from sham, 4T1, 4T1/sh control and 4T1/sh HMGB1 mice after sacrifice at day 15, fixed, decalcified and processed for subsequent histological analyses. Bone sections were incubated with rabbit anti-peripherin (1:100) antibody overnight at 4 C as primary antibodies, and then with donkey anti-rabbit IgG (1:100) as secondary antibody, followed by Alexa Fluor 488 anti-rabbit IgG (1:1000). Peripherin is a marker for SN. White asterisks in the figures indicate cortical bone. Peripherin$^+$ SNs were increased in the bone marrow of tibiae of 4T1 and 4T1/sh control mice compared to sham mice and decreased in the bone marrow of tibiae of 4T1/sh HMGB1 mice compared to 4T1 and 4T1/sh control mice. Scale bar 250 μm. (H) Quantitative evaluation of peripherin$^+$ SNs in the bone marrow of tibiae seen in Fig. 2G. Peripherin$^+$ fluorescent area and whole bone marrow area in histological sections were quantified under a fluorescent microscope using Neuron J software. Peripherin$^+$ SNs (%) on Y-axis in the figure was calculated as peripherin$^+$ fluorescent area/total bone marrow area ×100. Peripherin$^+$ SNs were increased in 4T1 mice, which was decreased by the treatment with HMGB1 antibody. Data are shown as mean ± SD (n = 8). * Significantly different from sham mice ($p < 0.05$). # Significantly different from 4T1 and 4T1/sh control mice ($p < 0.05$).

an antagonist for RAGE [30] on SN activity and BCABP in 4T1 mice to determine which receptor signal pathway is predominantly activated by HMGB1 to induce BCABP. The 4T1 mice showing BCABP were given a single intra-plantar injection of either TAK-242 or FPS-ZM1 at day 14 and evaluated for changes in BCABP. FPS-ZM1 reduced hind-paw mechanical hypersensitivity as early as 3 h after injection from 3.56 ± 0.39 g (Mean ± SD) to 5.18 ± 0.43 g (Mean ± SD), which lasted until 12 h (untreated vs FPS-ZM1 = 3.27 ± 0.19 g vs 5.22 ± 0.21 g) (Mean ± SD) and disappeared after 18 h (Fig. 3B). HMGB1 antibody also reduced hind-paw mechanical hypersensitivity 12 h after injection (untreated vs HMGB1 antibody = 3.27 ± 0.19 g vs 6.92 ± 0.65 g) (Mean ± SD), which lasted until 24 h (untreated vs HMGB1 antibody = 3.33 ± 0.15 g vs 6.38 ± 0.64 g) (Mean ± SD). Overall, HMGB1 antibody seemed to be more effective than FPS-ZM1 at relieving BCABP under this experimental conditions. In contrast, TAK-242 given on this experimental protocol showed little effects on BCABP. Further, FPS-ZM1 and HMGB1 antibody decreased pERK1/2 and pCREB in DRGs of 4T1 mice (Fig. 3C), while TAK-242 had no effects. These results suggest that HMGB1/RAGE axis is more predominant in the regulation of SN activity and induction of BCABP than HMGB1/TLR4. Role of TLR4 in BCABP needs further investigation. In addition, it should be noted that in this experiment, HMGB1 antibody and antagonists were given by only one single injection and BCABP was evaluated within 24 h. Under these circumstances, it is unlikely that 4T1 tumor burden in bone is changed. Thus, our results suggest that HMGB1 directly can regulate SN activity and BCABP independent of tumor burden.

3.4. Effects of HMGB1 secreted from 4T1 BC cells on DRG SN cells in vitro

To further determine the effects of HMGB1 produced by 4T1 BC on DRG SNs, we examined neurite outgrowth of F11 SN cells co-cultured with 4T1 BC cells in the absence or presence of the neutralizing antibody to HMGB1 in the microfluidic culture platforms. Few F11 SN cells cultured in the medium showed neurite outgrowth (Fig. 4A, left). In contrast, many F11 SN cells exhibited neurite outgrowth toward 4T1 BC cells in the co-culture (Fig. 4A, right). In agreement with these microscopic observations, the number of F11 SN cells with outgrowing neurites longer than 50 μm was considerably increased in the co-culture with 4T1 BC cells (Fig. 4B). Importantly, the neutralizing antibody to HMGB1 significantly decreased the number of F11 SN cells with neurite outgrowth by more than 50% (Fig. 4B). Control IgY antibody showed no effects.

We next determined the effects of the conditioned medium (CM) harvested from 4T1 BC cultures on neurite outgrowth of SN cells. Microscopic observation showed that 4T1 BC CM (20%, v/v) significantly increased F11 SN cells with outgrowing neurites (Fig. 4C). Assessment for the length of neurites extending from F11 SN cells revealed that F11 SN cells treated with 4T1 CM significantly have longer outgrowing neurites (Fig. 4D). These effects of 4T1 CM were blocked by the HMGB1 antibody by 60% (Fig. 4D). Dibutyryl cyclic AMP (DbcAMP, 1 mM), which served as a positive control, also increased neurite length of F11 SN cells. These results are in agreement with those obtained in 4T1 mice and suggest that 4T1 BC cells increase axogenesis of DRG SNs via secretion of HMGB1.

3.5. Role of HMGB1 in the progression of osteolysis associated with 4T1 BC colonization in bone

We next determined the role of HMGB1 in 4T1 BC colonization in bone. Radiological examination of osteolytic lesions to monitor 4T1 BC colonization in bone revealed that there are multiple osteolytic lesions in tibiae of 4T1 mice (Fig. 1B) and 4T1/sh control mice (Fig. 5A) and quantitative assessment for the area of these osteolytic lesions validated the radiographic results (Fig. 5B). In contrast, the area of osteolytic lesions was significantly decreased in 4T1/sh HMGB1 mice. Further, histological analysis demonstrated that the number of $TRAP^+$ OCs at tumor-bone interface at endocortical bone was increased (Fig. 5C). The number of $TRAP^+$ OCs per mm bone surface in tibiae was increased from 3.0 ± 1.0 (Mean ± SD) in sham mice to 65.67 ± 10.02 (Mean ± SD) in 4T1 mice and significantly decreased in tibiae of 4T1/sh HMGB1 mice to 42 ± 9.0 (Mean ± SD) (Fig. 5D). These results suggest that HMGB1 produced in 4T1 BC promoted osteoclastogenesis, leading to the development of bone destruction associated with 4T1 BC colonization.

In support of this notion, the CM (20%, v/v) harvested from 4T1 BC cultures increased the number of $TRAP^+$ MNOCs in bone marrow macrophage cultures (Fig. 5E). It should be noted that control and experimental groups were all treated with a suboptimal dose of M-CSF (30 ng/ml) and RANKL (10 ng/ml) in this experiment. To determine if increased osteoclastogenesis is due to HMGB1 secreted by 4T1 BC cells, the bone marrow macrophage cultures were treated with the CM of 4T1 BC in the absence or presence of increasing concentrations (10, 20 and 50 nM) of the RAGE antagonist FPS-ZM1 [31] or the TLR4 antagonist TAK-242 [29]. The experimental results showed that FPS-ZM1 dose-dependently and TAK-242 at 50 nM decreased 4T1 CM-increased osteoclastogenesis (Fig. 5F). These results collectively suggest that HMGB1 produced in 4T1 BC cells regulates the development and progression of osteoclastic bone destruction associated with 4T1 colonization in tibiae.

3.6. HMGB1 expression in human BCs

The results obtained in 4T1 mice led us to determine the pattern of HMGB1 expression in human BCs. Immunohistochemical analysis using human BC and normal breast tissue microarray showed that $HMGB1^+$ cells are significantly increased in human BCs compared to human normal breast tissues (Fig. 6A and 6B). These results suggest that HMGB1 contributes to BC tumorigenesis as previously reported [32].

HMGB1, which is a nuclear protein, is translocated to the cytoplasm prior to release into the extracellular space to exert its biological effects [10]. We therefore determined cytoplasmic and nuclear expression of HMGB1 in human BCs by immunohistochemistry (Fig. 6C). Of note, the percent of cells that express HMGB in the cytoplasm/cells that express HMGB1 in the cytoplasm and nucleus was significantly greater in BCs (60.3 ± 3.9%, Mean ± SD, n = 6) than normal breast tissues (29.8 ± 6.3%, Mean ± SD, n = 51) (Fig. 6D, right), while the percent of cells that express HMGB in the nucleus/cells that express HMGB1 in the cytoplasm and nucleus was equivalent between BCs and normal breast tissue (Fig. 6D, left). Taken together, these results suggest that translocation of HMGB1 from the nucleus to the cytoplasm may be critical for BC to induce BCABP.

4. Discussion

In this study we showed that HMGB1 secreted from intratibially-injected 4T1 BC cells induces BCABP in mice. HMGB1, which is a prototypic member of DAMPs, is secreted by a wide range of cancers and functions like a cytokine, creating an inflammatory cancer microenvironment [7]. Recent studies suggest that HMGB1 has both tumor-promoting and -suppressing effects during cancer development and treatment, acting as a double-edged sword [10]. In general, secreted HMGB1 is oncogenic by promoting proliferation, inflammation, energy metabolism, and angiogenesis

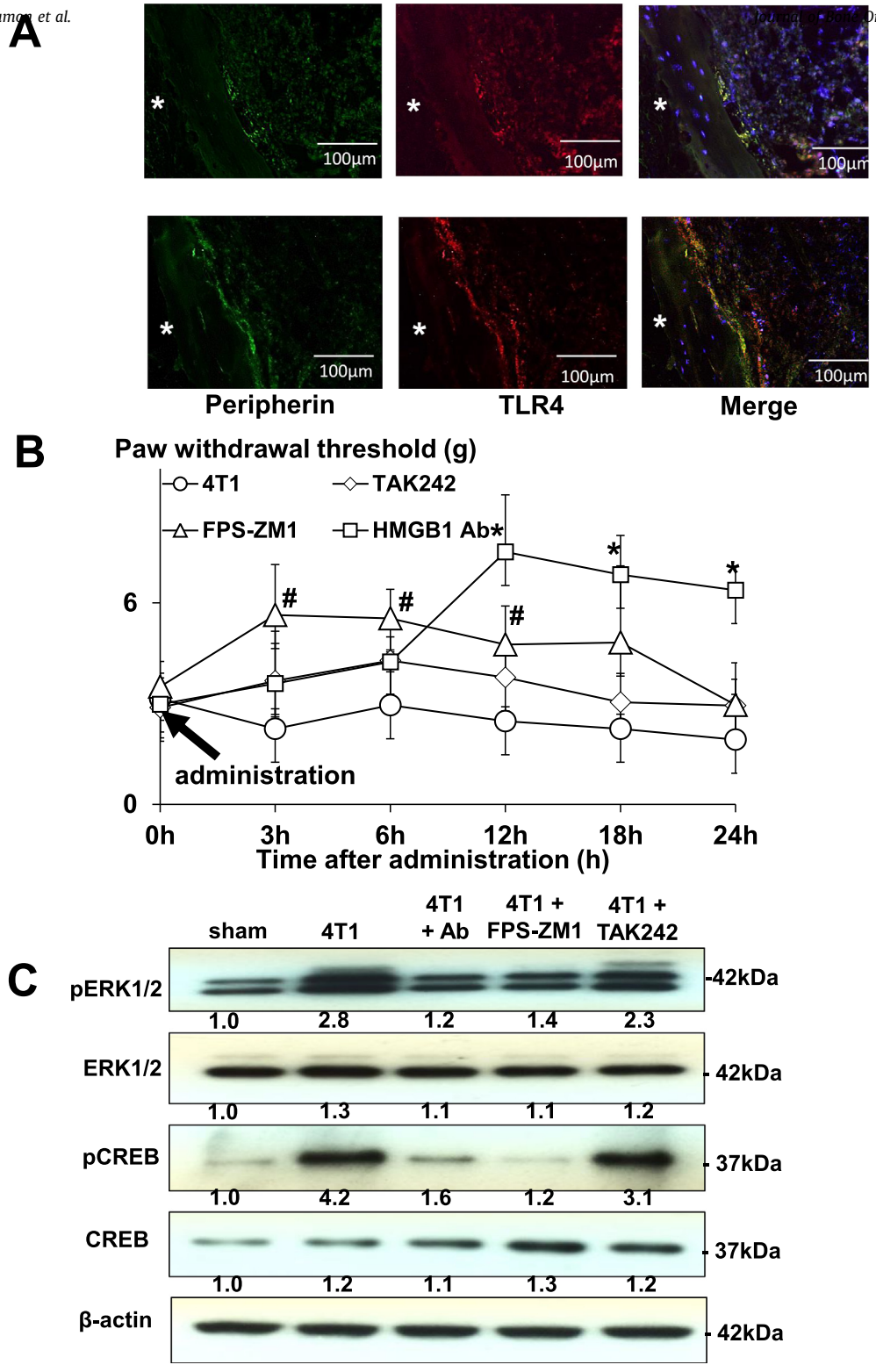

Fig. 3. Role of RAGE and TLR4 in BCABP. (A) Immunofluorochemical analysis of RAGE and TLR4 expression on peripherin^{+} SNs innervating bone. Bone sections were incubated with rabbit anti-peripherin (1:100), mouse anti-RAGE (1:100) and mouse anti-TLR4 (1:100) antibody at 4 C overnight as primary antibodies, followed by Alexa Fluor 488 anti-rabbit IgG (1:1000) and Alexa Fluor 647 anti-mouse IgG (1:1000) as secondary antibodies. Both RAGE and TLR4 were expressed on peripherin^{+} SNs innervating bone. White asterisks in the figures indicate cortical bone. Scale bar 100 μm. (B) Effects of pharmacological antagonist of RAGE and TLR4 on the progression of BCABP in 4T1 mice. One single intra-plantar injection of the RAGE antagonist, FPS-ZM1 (10 mg/kg/mouse), the TLR4 antagonist, TAK-242 (2 mg/kg/mouse), or the neutralizing antibody to HMGB1 (2 mg/kg/mouse) was given to 4T1 mice with BCABP at day 14 (arrow), and changes in hind-paw mechanical hypersensitivity of 4T1 mice were monitored by von Frey test 3, 6, 12, 18 and 24 h after antagonist and HMGB1 antibody injection. FPS-ZM1 reduced hind-paw mechanical hypersensitivity as early as 3 h after administration from 3.56 ± 0.39 g to 5.18 ± 0.43 g (Mean ± SD), which lasted until 12 h (untreated vs FPS-ZM1 = 3.27 ± 0.19 g vs 5.22 ± 0.21 g) (Mean ± SD) and disappeared after 18 h. HMGB1 antibody also reduced hind-paw mechanical hypersensitivity 12 h after injection (untreated vs HMGB1 antibody = 3.27 ± 0.19 g vs 6.92 ± 0.65 g) (Mean ± SD), which lasted until 24 h (untreated vs HMGB1 Antibody = 3.33 ± 0.15 g vs 6.38 ± 0.64 g) (Mean ± SD). Overall HMGB1 antibody appeared more effective than FPS-ZM1 at relieving BCABP under this experimental conditions. TAK-242 given on this experimental protocol showed no effects on BCABP. Data are shown as mean ± SD (n = 8 for each group). * Significantly different from 4T1 mice ($p < 0.01$). # Significantly different from 4T1 mice ($p < 0.05$). (C) Role of RAGE and TLR4 in the activation of SNs in DRGs of 4T1 mice. DRGs were harvested from 4T1 mice after 12 h treatment with vehicle, FPS-ZM1, TAK-242 and HMGB1 antibody, immediately lysed, and subjected to Western analysis. FPS-ZM1 and HMGB1 antibody decreased pERK1/2 and pCREB in DRGs of 4T1 mice, while TAK-242 had no effects.

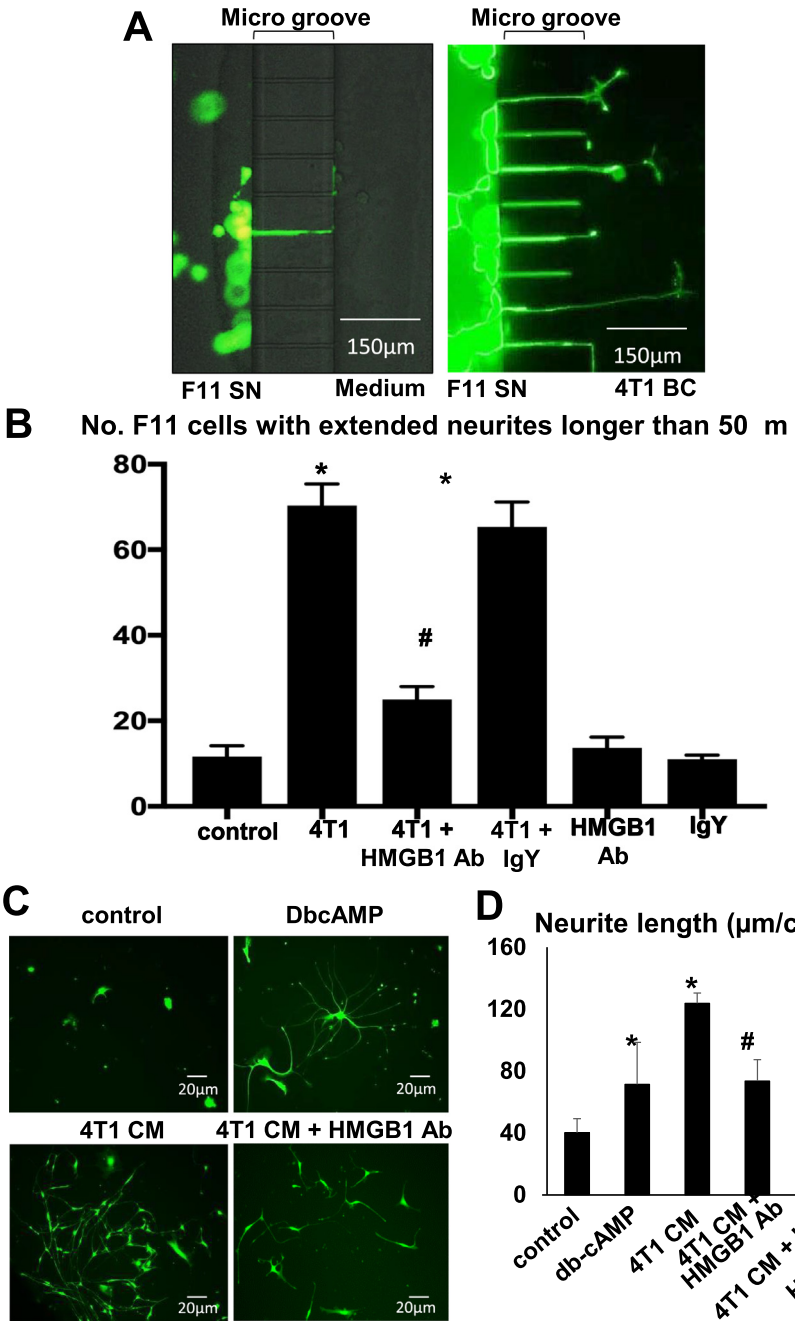

Fig. 4. Effects of HMGB1 secreted from4T1 BC cells on neurite outgrowth of DRG SN cells. (A) Effects of co-culture with 4T1 BC cells on neurite outgrowth of F11 SN cells in microfluidic culture platforms. F11 SN cells (10^5 cells, left chambers) were co-cultured with 4T1 BC cells (10^6 cells, right chambers) for 48 h in the absence or presence of the HMGB1 neutralizing antibody (50 μg/ml) or control IgY antibody. The chambers were then labeled with calcein AM (1 μM) for 10 min and F11 SN cells with extended neurites were observed under a fluorescent microscope. The number of F11 SN cells exhibiting extended neurite was increased in the co-cultures with 4T1 BC cells. Scale bar 150 μm. (B) Quantitative evaluation of neurite outgrowth in F11 SN cells in microfluidic culture platforms seen in Fig. 4A. F11 SN cells with extended neurite longer than 50 μm were counted under a fluorescent microscope using Neuron J software and are shown on Y-axis in the figure. The number of F11 SN cells with extended neurite is significantly increased in the co-cultures with 4T1 BC cells, and HMGB1 antibody significantly decreased the number. Data are shown as mean ± SD (n = 4). * Significantly different from medium control ($p < 0.05$). # Significantly different from 4T1 or 4T1 + IgY ($p < 0.05$). (C) Effects of CM harvested from 4T1 BC cell cultures on neurite outgrowth of F11 SN cells. F11 SN cells (10^4 cells/24-well plates) were treated with 4T1 BC cell CM (20%, v/v) in the neuron growth medium in the absence or presence of the neutralizing antibody to HMGB1 or control IgY antibody for 5 days. The plates were then stained with calcein AM (1 μM) for 10 min and observed under a fluorescent microscope. DbcAMP (1 mM) is a positive control. Scale bar 20 μm. (D) Quantitative evaluation of the effects of CM harvested from 4T1 BC cell cultures on neurite outgrowth of F11 SN cells. The length of all fluorescent neurites outgrowing from the cell body of F11 SN cells, and the number of all fluorescent cell body of F11 SN cells in plates were determined using Neuron J software under a fluorescent microscope. Neurite length (μm/cell) on Y-axis of the figure was calculated as, total length of all outgrowing neurites/number of total cell body of F11 SN cells. Neurite length of F11 SN cell expressed on Y-axis as μm per cell was increased to 123.73 ± 6.67 μm (Mean ± SD) by treatment with 4T1 CM, which is decreased to 37.61 ± 13.78 μm (Mean ± SD) by HMGB1 antibody. Data are shown as mean ± SD (n = 4). * Significantly different from medium control ($p < 0.05$). # Significantly different from 4T1 and 4T1 + IgY control antibody ($p < 0.05$).

and inhibiting host anticancer immunity. In contrast, intracellular HMGB1 has anti-tumor actions by stimulating the immunogenic cell death of cancer cells and stimulates anti-tumor immunity responses during chemo- or radio-therapy. Our results suggested that HMGB1 secreted from 4T1 BC cells is cancer-assisting by inducing BCABP, and increasing osteolytic lesions associated with

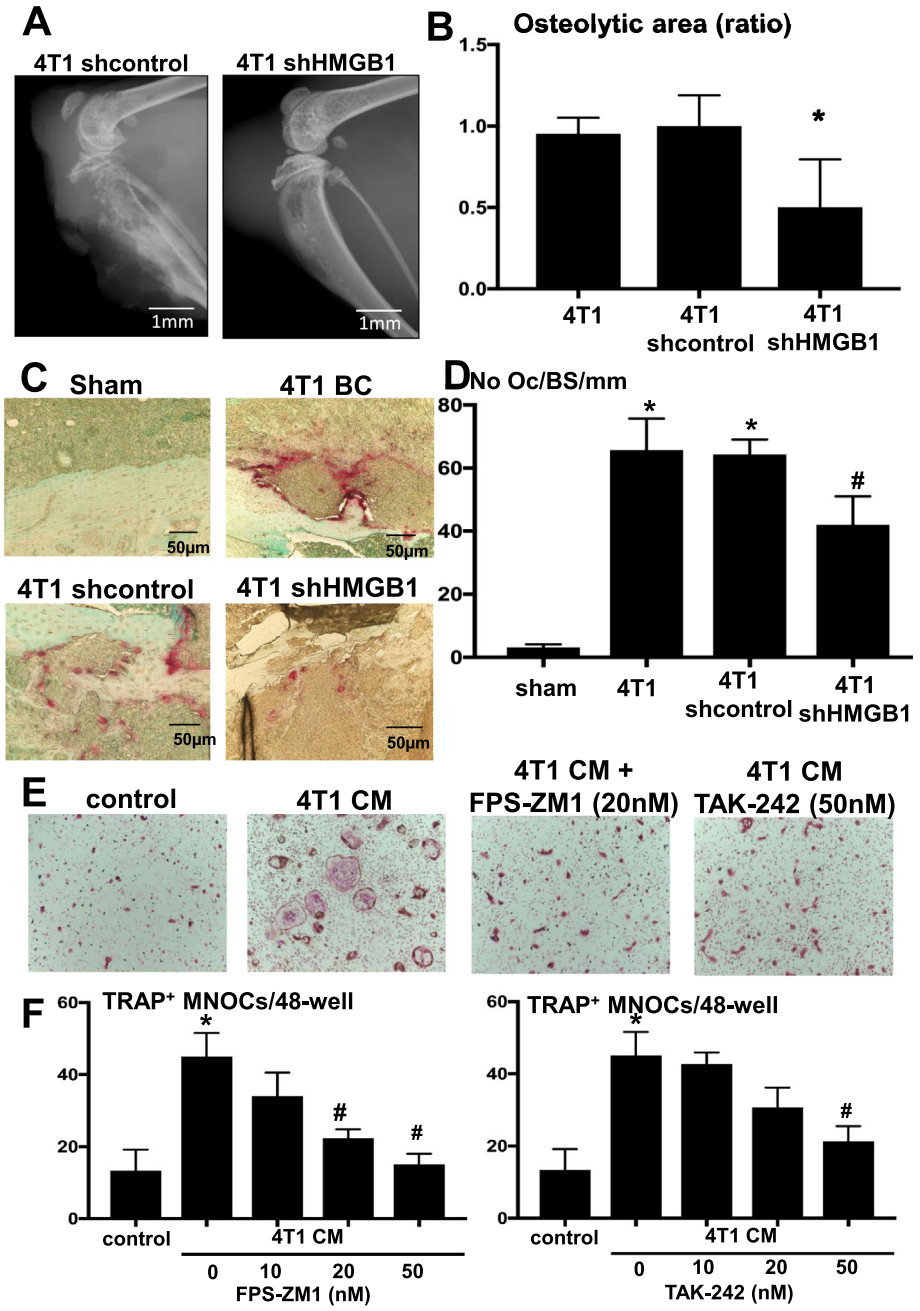

Fig. 5. Effects of HMGB1 on osteoclastic bone destruction associated with 4T1 BC colonization in tibiae. (A) Osteolytic lesions in tibiae of mice inoculated with 4T1/sh control (left) and 4T1/sh HMGB1 cells (right). Radiographs were taken at day 15 after intratibial cell inoculation (1×10^5 cells/10 μl). Scale bar 1 mm. (B) Quantitative evaluation of osteolytic lesions in tibiae of mice inoculated with 4T1/sh control and 4T1/sh HMGB1 cells seen in Fig. 4A. The area of osteoclastic bone destruction in tibiae was determined on radiographs using Image J. Osteolytic area (ratio) on Y-axis in the figure represents, area of 4T1/sh control or 4T1/sh HMGB1/area of 4T1 in which area of 4T1 is designated as 1. The area of osteolytic lesions associated with 4T1/sh HMGB1 cells were significantly smaller than those of 4T1 and 4T1/sh control. Data are shown as mean ± SD (n = 8). * Significantly different from sham control and 4T1/sh control mice ($p < 0.05$). (C) Histological pictures of the osteolytic lesions stained with TRAP. $TRAP^+$OCs at tumor-bone interface at endocortical bone are stained in red. Scale bar 50 μm. (D) Quantitative analysis of the number of $TRAP^+$ OCs formed in Fig. 4C. The number of OCs present at tumor-bone interface at endocortical bone was determined in three levels of histological sections for each sample under a microscope as described previously [24] and is shown on Y-axis as No OC/Bone Surface (BS)/mm in the figure. The number of $TRAP^+$OCs in osteolytic lesions associated with 4T1/sh HMGB1 cells was significantly less than that of 4T1 and 4T1/sh control. Data are shown as mean ± SD (n = 4). * Significantly different from sham mice ($p < 0.05$). # Significantly different from 4T1 mice and 4T1/sh control mice ($p < 0.05$). (E) Effects of 4T1 BC CM, FPS-ZM1 (RAGE antagonist) and TAK-242 (TLR4 antagonist) on $TRAP^+$MNOC formation. Bone marrow macrophages (1×10^5 cells/48-well) were cultured with or without 4T1 BC CM (20%, v/v) and in the absence or presence of FPS-ZM1 (20 nM) and TAK-242 (50 nM) with supplementation of suboptimal dose of M-CSF (30 ng/ml) and RANKL (10 ng/ml) for 5 days. Wells were then stained for TRAP. 4T1 BC CM increased $TRAP^+$MNOC formation, which was decreased by treatment with FPS-ZM1 and TAK-242. (F) Quantitative analysis of $TRAP^+$MNOC formation in bone marrow macrophage cultures seen in Fig. 4E. Cultures were treated with increasing doses (10, 20 and 50 nM) of FPS-ZM1 and TAK-242 for 5 days. The number of $TRAP^+$MNOCs was counted under a microscope. FPS-ZM1 significantly decreased $TRAP^+$MNOC formation in a dose-dependent manner, while TAK-242 significantly decreased it only at 50 nM. Data are shown as mean ± SD (n = 4). * Significantly different from control ($p < 0.01$).# Significantly different from 4T1 CM ($p < 0.05$). (For interpretation of the references to colour in this figure legend, the reader is referred to the web version of this article.)

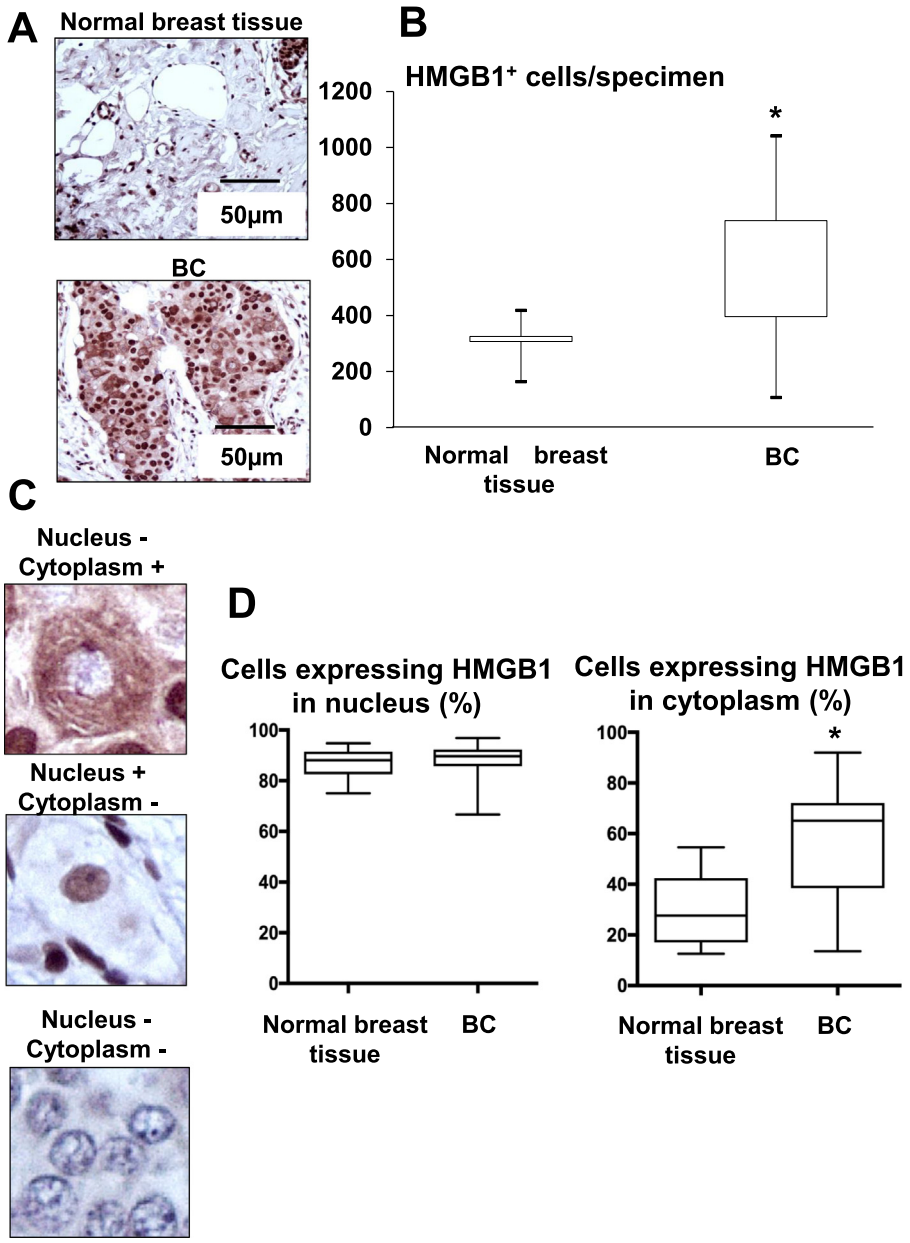

Fig. 6. Expression of HMGB1 in BCs using human tissue microarray. (A) Immunohistochemistry of HMGB1 expression in human normal breast tissue (top) and BC (bottom). Specimens were incubated with anti-HMGB1 antibody (1:100) overnight at 4 °C, followed by the treatment with streptoavidin-biotin complex (1:100) for 60 min, and visualized with the use of a DAB substrate-chromogen solution. HMGB1-positive cells are stained in brown. Scale bar 50 μm. (B) Number of HMGB1-positive cells in human normal breast tissue (n = 6) and BC (n = 51). HMGB1$^+$ cells on specimens were counted using a BZ-X800 analyzer hybrid cell count system, and the relative integrated density was calculated as number of HMGB1$^+$ cells/specimen as shown on Y-axis in the figure. Data are shown as mean ± SD. * Significantly different from normal breast tissue ($p < 0.001$). (C) BC cell with HMGB1-negative in nucleus and -positive in cytoplasm (top), HMGB1-positive in nucleus and -negative in cytoplasm (middle), and HMGB1-negative in nucleus and -negative in cytoplasm (bottom). (D) Expression of HMGB1 in nucleus (left) and cytoplasm (right) in normal breast tissues (n = 6) and BC (n = 51). Cells expressing HMGB1 in nucleus and cytoplasm in normal breast tissues and BC were counted. Y-axis in the figure indicates as, the percent of cells that express HMGB in the nucleus/cells that express HMGB1 in the cytoplasm and nucleus ×100 (left), and the percent of cells that express HMGB in the cytoplasm/cells that express HMGB1 in the cytoplasm and nucleus ×100 (right). The percent of cells expressing HMGB in the cytoplasm was significantly greater in BCs than normal breast tissues (Fig. 6D, right), while the percent of cells expressing HMGB in the nucleus was not different between BCs and normal breast tissue (Fig. 6D, left). Data are mean ± SD. * Significantly different from normal breast tissue ($p < 0.001$).

4T1 BC colonization in bone. Importantly, we showed that the neutralizing antibody to HMGB1 significantly decreased these actions of HMGB1. These results suggest that blocking the cytokine-like actions of secreted HMGB1 may be a therapeutic approach for the management of BCABP and bone metastasis.

Biological actions of extracellular HMGB1 are elicited through binding to several cell surface receptors expressed on target tissues and cells. RAGE and TLR4 are two of the major receptors that mediate the biological actions of HMGB1. However, functional discrimination if RAGE and TLR4 or both are involved in many of HMGB1's actions in inflammation, immunity and cancer development and progression still remains debatable. In this study, we showed that both RAGE and TLR4 are expressed on peripherin$^+$ SNs innervating bone and found that FPS-ZM1, a selective RAGE antagonist, but not TAK242, a selective TLR4 antagonist, reduced BCABP. These results suggest that RAGE rather than TLR4 mediates

HMGB1-induced BCABP. In fact, propagation of downstream signaling pathways of RAGE following HMGB1 binding leads to the activation of the molecular pain markers, ERK1/2 and CREB [33]. Thus, HMGB1/RAGE/ERK1/2/CREB axis is likely a predominant signaling pathway that leads to the induction of BCABP. Further study will warrant to define the role of HMGB1/RAGE axis in the regulation of neuronal reactions in response to cancer colonization in bone.

A previous study described that HMGB1 increases RANKL-induced osteoclastogenesis via activating RAGE, but not TRL4, signaling [34]. Osteoclasts are a key player in the pathophysiology of osteolytic bone metastasis [35]. We therefore determined if HMGB1 derived 4T1 BC cells regulates osteolysis associated with 4T1 BC colonization in bone. Our radiological and histological analyses showed decreased area of osteolytic lesions and reduced number of $TRAP^{+}$ osteoclasts in tibiae of 4T1/sh HMGB1 mice compared to 4T1 mice and 4T1/sh control mice. These results together with an earlier report [34] indicate a crucial role of HMGB1 produced in cancer in the development and progression of osteolytic bone metastasis.

Our result that RANKL-induced osteoclastogenesis is enhanced by HMGB1/RAGE axis, and accumulating data that osteoclasts contribute to the induction of BCABP by releasing protons to degrade bone minerals during bone resorption [2,28] together suggest that reduced BCABP by administration of the neutralizing antibody to HMGB1 and antagonists to RAGE and TLR4 to 4T1 mice is partially due to decreased proton secretion from suppressed osteoclasts. In fact, the specific inhibitors of osteoclasts, bisphosphonates and denosumab, are shown to effectively improve BCABP in breast cancer patients [36]. However, in this study, the HMGB1 antibody and RAGE antagonist FPS-ZM1 and TLR4 antagonist TAK-242 were given to 4T1 mice only by one single injection and reduction of BCABP emerged 3 h for FPS-ZM1 and 12 h for HMGB1 antibody following agent administration. It is thus unlikely, we suspect, that bone resorption is inhibited within 3 to 12 h, leading to reduced BCABP under these circumstances. Thus, HMGB1, RAGE and TLR4 play a role in the induction of BCABP via not only osteoclast-associated mechanism but also direct activation of SNs.

In this study we found the expression of HMGB1 in human BCs is increased compared with that in normal human breast tissue. Further, our results also show that cytoplasmic expression of HMGB1 is significantly greater in BCs than in normal breast tissue. HMGB1 primarily is a structural protein of chromatin in the nucleus that functions as a DNA chaperone, regulating nuclear homeostasis and genome stability [10]. However, HMGB1 is actively secreted into the extracellular environments following translocation from the nucleus to the cytoplasm in response to endogenous and exogenous stimuli [33]. It has been proposed that post-translational modifications of HMGB1 by acetylation, phosphorylation, methylation and poly (ADP)-ribosylation promote the translocation of HMGB1 from the nucleus to the cytoplasm, leading to the secretion of HMGB1. Further, increased apoptosis in cancer cells due to anti-cancer chemotherapy and radiation also promotes HMGB1 release [10]. Although we did not investigate the mechanism of increased cytoplasmic expression of HMGB1 in human BC cells in this study, our results suggest that BC cells may have the intrinsic intracellular machinery by which HMGB1 is produced in increased levels in the nucleus, translocated to the cytoplasm, and consequently secreted into the extracellular environments, thereby promoting the aggressiveness of BC and inducing associated complications such as bone pain.

Bone is relatively hypoxic compared to other organs [37] and hypoxia is a potent stimulator of HMGB1 secretion from cancer cells [8], collectively suggesting that HMGB1 levels are likely up-regulated in cancer bone metastasis. Further, bone is densely innervated by SNs [38]. Thus, bone provides a unique microenvironment in which HMGB1 contributes to the pathophysiology of BCABP induced via the interactions between bone metastatic cancer cells and SNs. Recently, HMGB1/RAGE is found to be involved in skeletal development, homeostasis, repair and regeneration via regulation of functions of the cellular components of bone microenvironment including osteocytes, osteoblasts and osteoclasts [39]. Our results suggest that SNs are an additional component of bone microenvironment regulated by the HMGB1/RAGE axis, interacting with metastatic BC in the pathophysiology of BCABP in bone microenvironment.

In conclusion, our study demonstrates that BC secretes HMGB1 to induce BCABP by activating RAGE signaling in SNs innervating bone. We propose that HMGB1/RAGE axis may be a novel therapeutic target for BCABP, as well as a potential biomarker for BCABP.

CRediT authorship contribution statement

Tatsuo Okui: Investigation, Data curation, Formal analysis. **Masahiro Hiasa:** Validation, Investigation. **Shoji Ryumon:** Visualization, Investigation. **Kisho Ono:** Visualization, Investigation. **Yuki Kunisada:** Visualization, Investigation. **Soichiro Ibaragi:** . **Akira Sasaki:** Methodology, Supervision. **G. David Roodman:** Methodology, Supervision. **Fletcher A. White:** Methodology, Supervision. **Toshiyuki Yoneda:** Conceptualization, Supervision, Resources, Methodology.

Declaration of Competing Interest

The authors declare that they have no known competing financial interests or personal relationships that could have appeared to influence the work reported in this paper.

Acknowledgements

This study is supported by the Project Development Team within the ICTSI NIH/NCRR (#TR000006), the Grant-in-Aid for Young Scientists (JSPS: Japan Society for the Promotion of Science Indiana University School of Medicine, USA KAKENHI grant no. 18K17225) to TO, the Grants-in-Aid for Scientific Research (JSPS KAKENHI grant no. 17H04377, 20H03859) to TY, the IU Health Strategic Research Initiative in Oncology, and start-up fund of Indiana University School of Medicine to TY, Merit Review Funds from the Veterans Administration to GDR, and the NIH (#DK100905), MERIT Review Award (#BX002209) from the U.S. Department of Veterans Affairs to FAW, and Japan Society for the Promotion of Science Grants-in-aid for Research Activity Start-up and Postdoctoral Fellowship for Research Abroad to TO.

References

[1] M.J. Goblirsch, P.P. Zwolak, D.R. Clohisy, Biology of bone cancer pain, Clin. Cancer Res. 12 (20 Pt 2) (2006) 6231s–6235s.
[2] P.W. Mantyh, Cancer pain and its impact on diagnosis, survival and quality of life, Nat. Rev. Neurosci. 7 (10) (2006) 797–809.
[3] G. Schneider, R. Voltz, J. Gaertner, Cancer pain management and bone metastases: an update for the clinician, Breast Care (Basel) 7 (2) (2012) 113–120.
[4] S. Dalal, E. Bruera, Access to opioid analgesics and pain relief for patients with cancer, Nat. Rev. Clin. Oncol. 10 (2) (2013) 108–116.
[5] J.C. Ballantyne, K.S. LaForge, Opioid dependence and addiction during opioid treatment of chronic pain, Pain 129 (3) (2007) 235–255.
[6] S. Falk, A.H. Dickenson, Pain and nociception: mechanisms of cancer-induced bone pain, J. Clin. Oncol. 32 (16) (2014) 1647–1654.
[7] C. Hernandez, P. Huebener, R.F. Schwabe, Damage-associated molecular patterns in cancer: a double-edged sword, Oncogene 35 (46) (2016) 5931–5941.
[8] A.D. Garg, P. Agostinis, Cell death and immunity in cancer: From danger signals to mimicry of pathogen defense responses, Immunol. Rev. 280 (1) (2017) 126–148.

[9] M. Carballo, P. Puigdomenech, J. Palau, DNA and histone H1 interact with different domains of HMG 1 and 2 proteins, EMBO J. 2 (10) (1983) 1759–1764.
[10] R. Kang, Q. Zhang, H.J. Zeh 3rd, M.T. Lotze, D. Tang, HMGB1 in cancer: good, bad, or both?, Clin. Cancer Res. 19 (15) (2013) 4046–4057.
[11] S. Sun, W. Zhang, Z. Cui, Q. Chen, P. Xie, C. Zhou, B. Liu, X. Peng, Y. Zhang, High mobility group box-1 and its clinical value in breast cancer, Onco Targets Ther 8 (2015) 413–419.
[12] L.L. Man, F. Liu, Y.J. Wang, H.H. Song, H.B. Xu, Z.W. Zhu, Q. Zhang, Y.J. Wang, The HMGB1 signaling pathway activates the inflammatory response in Schwann cells, Neural Regen. Res. 10 (10) (2015) 1706–1712.
[13] N. Das, V. Dewan, P.M. Grace, R.J. Gunn, R. Tamura, N. Tzarum, L.R. Watkins, I.A. Wilson, H. Yin, HMGB1 activates proinflammatory signaling via TLR5 leading to allodynia, Cell Rep. 17 (4) (2016) 1128–1140.
[14] G.L. Currie, A. Delaney, M.I. Bennett, A.H. Dickenson, K.J. Egan, H.M. Vesterinen, E.S. Sena, M.R. Macleod, L.A. Colvin, M.T. Fallon, Animal models of bone cancer pain: systematic review and meta-analyses, Pain 154 (6) (2013) 917–926.
[15] Y. Kawasaki, T. Kohno, Z.Y. Zhuang, G.J. Brenner, H. Wang, C. Van Der Meer, K. Befort, C.J. Woolf, R.R. Ji, Ionotropic and metabotropic receptors, protein kinase A, protein kinase C, and Src contribute to C-fiber-induced ERK activation and cAMP response element-binding protein phosphorylation in dorsal horn neurons, leading to central sensitization, J. Neurosci. 24 (38) (2004) 8310–8321.
[16] M. Nakanishi, K. Hata, T. Nagayama, T. Sakurai, T. Nishisho, H. Wakabayashi, T. Hiraga, S. Ebisu, T. Yoneda, Acid activation of Trpv1 leads to an up-regulation of calcitonin gene-related peptide expression in dorsal root ganglion neurons via the CaMK-CREB cascade: a potential mechanism of inflammatory pain, Mol. Biol. Cell 21 (15) (2010) 2568–2577.
[17] W. Chen, R. Mi, N. Haughey, M. Oz, A. Höke, Immortalization and characterization of a nociceptive dorsal root ganglion sensory neuronal line, J. Peripher. Nerv. Syst. 12 (2) (2007) 121–130.
[18] E. Meijering, Neuron tracing in perspective, Cytometry A 77 (7) (2010) 693–704.
[19] A.M. Taylor, M. Blurton-Jones, S.W. Rhee, D.H. Cribbs, C.W. Cotman, N.L. Jeon, A microfluidic culture platform for CNS axonal injury, regeneration and transport, Nat. Methods 2 (8) (2005) 599–605.
[20] A. Morisawa, T. Okui, T. Shimo, S. Ibaragi, Y. Okusha, M. Ono, T.T.H. Nguyen, N. M.M. Hassan, A. Sasaki, Ammonium tetrathiomolybdate enhances the antitumor effects of cetuximab via the suppression of osteoclastogenesis in head and neck squamous carcinoma, Int. J. Oncol. 52 (3) (2018) 989–999.
[21] K. Hasegawa, T. Okui, T. Shimo, S. Ibaragi, H. Kawai, S. Ryumon, K. Kishimoto, Y. Okusha, N.M. Monsur Hassan, A. Sasaki, Lactate transporter monocarboxylate transporter 4 induces bone pain in head and neck squamous cell carcinoma, Int. J. Mol. Sci. 19 (11) (2018).
[22] T. Okui, T. Shimo, T. Fukazawa, N. Kurio, N.M. Hassan, T. Honami, M. Takaoka, Y. Naomoto, A. Sasaki, Antitumor effect of temsirolimus against oral squamous cell carcinoma associated with bone destruction, Mol. Cancer Ther. 9 (11) (2010) 2960–2969.
[23] M. Hiasa, T. Okui, Y.M. Allette, M.S. Ripsch, G.H. Sun-Wada, H. Wakabayashi, G. D. Roodman, F.A. White, T. Yoneda, Bone pain induced by multiple myeloma is reduced by targeting V-ATPase and ASIC3, Cancer Res. 77 (6) (2017) 1283–1295.
[24] T. Hiraga, S. Ito, H. Nakamura, Cancer stem-like cell marker CD44 promotes bone metastases by enhancing tumorigenicity, cell motility, and hyaluronan production, Cancer Res. 73 (13) (2013) 4112–4122.
[25] I. Masouris, M. Klein, S. Dyckhoff, B. Angele, H.W. Pfister, U. Koedel, Inhibition of DAMP signaling as an effective adjunctive treatment strategy in pneumococcal meningitis, J. Neuroinflamm. 14 (1) (2017) 214.
[26] M. Tsubota, R. Fukuda, Y. Hayashi, T. Miyazaki, S. Ueda, R. Yamashita, N. Koike, F. Sekiguchi, H. Wake, S. Wakatsuki, Y. Ujiie, T. Araki, M. Nishibori, A. Kawabata, Role of non-macrophage cell-derived HMGB1 in oxaliplatin-induced peripheral neuropathy and its prevention by the thrombin/thrombomodulin system in rodents: negative impact of anticoagulants, J. Neuroinflamm. 16 (1) (2019) 199.
[27] C. Yoshihara-Hirata, K. Yamashiro, T. Yamamoto, H. Aoyagi, H. Ideguchi, M. Kawamura, R. Suzuki, M. Ono, H. Wake, M. Nishibori, S. Takashiba, Anti-HMGB1 neutralizing antibody attenuates periodontal inflammation and bone resorption in a murine periodontitis model, Infect. Immun. 86 (5) (2018).
[28] T. Yoneda, M. Hiasa, T. Okui, Crosstalk between sensory nerves and cancer in bone, Curr. Osteoporos. Rep. 16 (6) (2018) 648–656.
[29] S.A. Woller, S.B. Ravula, F.C. Tucci, G. Beaton, M. Corr, R.R. Isseroff, A.M. Soulika, M. Chigbrow, K.A. Eddinger, T.L. Yaksh, Systemic TAK-242 prevents intrathecal LPS evoked hyperalgesia in male, but not female mice and prevents delayed allodynia following intraplantar formalin in both male and female mice: the role of TLR4 in the evolution of a persistent pain state, Brain Behav. Immun. 56 (2016) 271–280.
[30] F. Ma, D.E. Kouzoukas, K.L. Meyer-Siegler, K.N. Westlund, D.E. Hunt, P.L. Vera, Disulfide high mobility group box-1 causes bladder pain through bladder Toll-like receptor 4, BMC Physiol. 17 (1) (2017) 6.
[31] R. Deane, I. Singh, A.P. Sagare, R.D. Bell, N.T. Ross, B. LaRue, R. Love, S. Perry, N. Paquette, R.J. Deane, M. Thiyagarajan, T. Zarcone, G. Fritz, A.E. Friedman, B.L. Miller, B.V. Zlokovic, A multimodal RAGE-specific inhibitor reduces amyloid β-mediated brain disorder in a mouse model of Alzheimer disease, J. Clin. Invest. 122 (4) (2012) 1377–1392.
[32] Y. Sun, Y. Tu, L.I. He, C. Ji, B.O. Cheng, High mobility group box 1 regulates tumor metastasis in cutaneous squamous cell carcinoma via the PI3K/AKT and MAPK signaling pathways, Oncol. Lett. 11 (1) (2016) 59–62.
[33] H. Rauvala, A. Rouhiainen, Physiological and pathophysiological outcomes of the interactions of HMGB1 with cell surface receptors, Biochim. Biophys. Acta 1799 (1–2) (2010) 164–170.
[34] Z. Zhou, J.Y. Han, C.X. Xi, J.X. Xie, X. Feng, C.Y. Wang, L. Mei, W.C. Xiong, HMGB1 regulates RANKL-induced osteoclastogenesis in a manner dependent on RAGE, J. Bone Miner. Res. 23 (7) (2008) 1084–1096.
[35] K.N. Weilbaecher, T.A. Guise, L.K. McCauley, Cancer to bone: a fatal attraction, Nat. Rev. Cancer 11 (6) (2011) 411–425.
[36] C.S. Cleeland, J.J. Body, A. Stopeck, R. von Moos, L. Fallowfield, S.D. Mathias, D.L. Patrick, M. Clemons, K. Tonkin, N. Masuda, A. Lipton, R. de Boer, S. Salvagni, C.T. Oliveira, Y. Qian, Q. Jiang, R. Dansey, A. Braun, K. Chung, Pain outcomes in patients with advanced breast cancer and bone metastases: results from a randomized, double-blind study of denosumab and zoledronic acid, Cancer 119 (4) (2013) 832–838.
[37] E. Schipani, C. Maes, G. Carmeliet, G.L. Semenza, Regulation of osteogenesis-angiogenesis coupling by HIFs and VEGF, J. Bone Miner. Res. 24 (8) (2009) 1347–1353.
[38] D.B. Mach, S.D. Rogers, M.C. Sabino, N.M. Luger, M.J. Schwei, J.D. Pomonis, C.P. Keyser, D.R. Clohisy, D.J. Adams, P. O'Leary, P.W. Mantyh, Origins of skeletal pain: sensory and sympathetic innervation of the mouse femur, Neuroscience 113 (1) (2002) 155–166.
[39] L.I. Plotkin, A.L. Essex, H.M. Davis, RAGE signaling in skeletal biology, Curr. Osteoporos. Rep. 17 (1) (2019) 16–25.